

Inversion of multiangle sky radiance measurements for the retrieval of atmospheric optical properties

1. Algorithm

Yi Qin and Michael A. Box

School of Physics, University of New South Wales, Sydney, New South Wales, Australia

David L. B. Jupp

Earth Observation Center, CSIRO, Canberra, ACT, Australia

Received 14 June 2001; revised 20 March 2002; accepted 13 June 2002; published 27 November 2002.

[1] An inversion technique is developed that retrieves single scattering albedo and phase function from multiangle sky radiance measured at the ground. A linear equation system is first derived from the radiative perturbation theory to approximately represent exiting radiance as a function of single scattering albedo and the Legendre polynomial coefficients of the phase function. However, this linear system is ill-posed. Regularization is thus introduced to obtain a stable solution. An important and difficult step of the regularization is the determination of the regularization parameter, especially when iteration is involved in the inversion. A number of methods described in the literature that fit best into our general inversion approach, such as the L curve method, have been tried, but it is found that the regularization parameter derived from these methods is constantly too small, resulting in an unstable inversion procedure. Because of this, efforts have been made to obtain a more appropriate regularization parameter. In this paper, we focus on the development of the inversion technique. Results obtained using the technique from both synthetic and real measurements are presented by *Qin et al.* [2002b].

INDEX TERMS: 0305 Atmospheric Composition and Structure: Aerosols and particles (0345, 4801); 3359 Meteorology and Atmospheric Dynamics: Radiative processes; 0360 Atmospheric Composition and Structure: Transmission and scattering of radiation; 0394 Atmospheric Composition and Structure: Instruments and techniques; *KEYWORDS:* aerosols, single scattering albedo, phase function, retrieval

Citation: Qin, Y., M. A. Box, and D. L. B. Jupp, Inversion of multiangle sky radiance measurements for the retrieval of atmospheric optical properties, 1, Algorithm, *J. Geophys. Res.*, 107(D22), 4652, doi:10.1029/2001JD000945, 2002.

1. Introduction

[2] Atmospheric optical properties are of great interest to satellite remote sensing data validation [Holben *et al.*, 1992], climate forcing [Charlson *et al.*, 1992], and to virtually anyone who is concerned with atmospheric radiative transfer. Multiangle sky radiance and direct solar radiance measurements, such as supplied by the AERONET network [Holben *et al.*, 1998], have provided the opportunity to derive the full set of optical properties, including the scattering phase function and single scattering albedo, as well as the optical thickness. Due to the great interest in these parameters, a lot of effort has been made to retrieve them. Among them, the following are most relevant to this paper. The algorithm proposed by Wang and Gordon [1993] and Yang and Gordon [1998] retrieves the optical properties directly. The technique proposed by Dubovik *et al.* [2000] and Dubovik and King [2000], which has been widely applied, especially to the AERONET data, retrieves aerosol size distribution and refractive index. The optical param-

eters can then be reconstructed, on the assumption of spherical particles as used by Mie theory. The method proposed by Nakajima *et al.* [1996] also retrieves the aerosol size distribution and is also widely used at AERONET stations.

[3] On the basis of earlier work by Box and Sendra [1999] and Sendra and Box [2000], in this paper an inversion procedure will be presented to retrieve the column single scattering albedo and phase function from multiangle sky radiance measured at the ground. As with the method of Wang and Gordon [1993] and Yang and Gordon [1998], our method also retrieves the optical parameters directly. Because Mie theory is not involved directly in the inversions, no assumption has been made about the shape of the aerosol particles. The largest difference between the two methods is that our approach retrieves the Legendre polynomial coefficients of the phase function rather than the phase function itself. This approach is implemented by firstly linearizing approximately the radiative transfer equation using the radiative perturbation theory [Box *et al.*, 1989a]. Unfortunately the derived linear equation system is ill-posed. This paper will introduce regularization techniques to overcome the difficulties in solving such problems.

As will be shown in this paper, because the phase function coefficients have a closer and direct connection with aerosol size distribution and refractive index, this approach could be a good basis for further retrieval of the physical parameters of aerosols.

[4] First, in section 2, we derive an approximate linear system from the radiative transfer equation and introduce the overall approach to solve this system, then the ill posedness of the system is discussed and a regularization method is introduced in section 3. In section 4, we discuss the development of the regularization algorithm, including the smoothing matrix, the trial solution and the regularization parameter. In section 5, we sum up the discussions. Inversion results using the developed method, as well as a sensitivity study, will be presented in another paper.

2. Linear Representation of Radiance Perturbation and the Overall Inversion Approach

[5] In this section, we briefly derive a linear equation system that approximately represents the relation between the radiances and the optical parameters. By applying the radiative adjoint formulation [Box *et al.*, 1988], it has been shown [Box *et al.*, 1989a, 1997; Box, 2002] that any perturbation (variation) of a given radiative effect, ΔE , such as the perturbation of radiative intensity or fluxes, can be expressed as

$$\Delta E = E - E_0 = -\langle I^+, \Delta LI_0 \rangle = -\langle I_0^+, \Delta LI \rangle, \quad (1)$$

where L , I are respectively the radiative transfer operator and the intensity. In this equation, the superscript plus denotes the ‘‘adjoint,’’ and the subscript zero denotes a base atmospheric model relative to which any perturbation values are calculated. $\langle A, B \rangle$ denotes the integration of AB over the altitude, zenith, and azimuth.

[6] To a first-order approximation, I^+ was substituted by I_0^+ , or I substituted by I_0 , and hence [Box *et al.*, 1989a]

$$\Delta E \approx -\langle I_0^+, \Delta LI_0 \rangle. \quad (2)$$

One direct application of equation (2) is in the efficient calculation of multiple radiative effects [Box *et al.*, 1989b]. However, in this paper, this equation will be used inversely. That is, we intend to invert equation (2) to retrieve atmospheric optical properties from measured sky radiances. To achieve this, equation (2) has to be expanded so that sky radiance is explicitly expressed as function of the properties to be retrieved. This is done by expanding the intensity, I_0 , and the adjoint intensity, I_0^+ , into cosine series, and the phase function, P , (which is implicitly included in the radiative transfer operator, L) into a series of Legendre polynomials. This procedure is exactly the same as the derivation of the discrete-ordinates algorithm for solving the plane parallel atmospheric radiative transfer equation [Liou, 1980]. It is also of particular interest to us because a discrete-ordinates algorithm based radiative transfer code has been used throughout this work to perform all the relevant calculations, which allows for special consideration being taken to greatly improve the efficiency of computation [Qin *et al.*, 2002a]. Assuming the phase function and

single scattering albedo are independent of altitude and substituting the expanded intensity, adjoint intensity, and phase function into equation (2), it has been shown that [Sendra, 1996; Sendra and Box, 2000]:

$$\Delta I \approx A_1 \Delta \sigma_t + \sum_{l=0}^{N-1} A_{2l} \Delta \eta_l. \quad (3)$$

Because of this assumption, the phase function and single scattering albedo thus retrieved are the column phase function and column single scattering albedo. In equation (3),

$$\begin{aligned} \Delta I &= I - I_0, \\ \Delta \sigma_t &= \sigma_t - \sigma_{t0}, \\ \Delta \eta_l &= \sigma_s \chi_l - \sigma_{s0} \chi_{l0}. \end{aligned} \quad (4)$$

Again, subscript zero denotes a base model; σ_t is the extinction cross section of the atmosphere, σ_s is the scattering cross section, χ_l are the coefficients of the expanded phase function and are referred to as the phase function coefficients hereafter. These parameters are defined as

$$P(\Theta) = \sum_{l=0}^{2N_t-1} \chi_l P_l(\cos(\Theta)). \quad (5)$$

A_1 and A_2 , hereinafter referred as the first and second kernel, are calculated solely from the base model. A revised version of their calculation is given by Qin *et al.* [2002a] in the second paper of this series.

[7] In this paper, we will be concentrating on ground-based measurements. In this case, the extinction cross section (in fact the optical thickness) can be deduced, with predictable error, from direct solar radiance measurements. Because of this, we assume $\sigma_{t0} = \sigma_t$ or $\Delta \sigma_t = 0$. Only the single scattering albedo and phase function will be retrieved in the inversion. We also assume that the surface reflection model is known. A sensitivity analysis will be given by Qin *et al.* [2002b] regarding these assumptions.

[8] When a number of intensities are measured at different angles, equation (3) yields a linear system which may be written as

$$\begin{aligned} \Delta \mathbf{I} &= \mathbf{A} \Delta \boldsymbol{\eta} \\ \Delta \mathbf{I} &= \Delta \bar{\mathbf{I}} + \boldsymbol{\varepsilon}, \end{aligned} \quad (6)$$

where \mathbf{A} is a real matrix of dimension M (the number of measurements) by N (the number of parameters to be inverted). $\Delta \boldsymbol{\eta}$ is an N -element vector. $\Delta \mathbf{I}$, the differences between the measured and base model (or first guess) radiances, and $\Delta \bar{\mathbf{I}}$, the true (error free) radiance differences, are both M -element vectors. In equation (6) the term $\boldsymbol{\varepsilon}$ describes all the error sources. Among them are the measurement error, kernel approximation error, and phase function truncation error.

[9] Because of the phase function expansion, only a limited number of terms might be used which could cause significant truncation error. In this paper, we will always use sufficient phase function terms so that the truncation error can be ignored. In a subsequent work we wish to model high-order terms (which mainly contribute to the most

forward part of the scattering), so that we may still be able to retrieve the lower-order terms even when the number of phase function terms is not large enough; for example, when very large particles dominate and it becomes impractical to use a very large set of phase function coefficients. Note that it is the low-order expansion coefficients which are most important for computation of radiative forcing by aerosols.

[10] Because of the fact that the derived linear equation system is an approximate system, i.e., the coefficient matrix, \mathbf{A} , in equation (6) is derived from an initial base atmospheric model, iteration will be used to solve the system. In each iteration, the base model is upgraded using the newly solved parameters, $\Delta\boldsymbol{\eta}$, and the coefficient matrix is recalculated. *Qin et al.* [2002b] will show that the iteration usually converges very rapidly. This is due to the merit of the perturbation theory which, as well as considering the single scattering component exactly, considers the multiple scattering component approximately [*Qin et al.*, 2002a]. Having set up this overall approach, we will concentrate on the solving of equation (6) in the remainder of this paper.

3. The Ill-Posed Problem and the Regularization Approaches

3.1. The General Form of Philips–Twomey–Tikhonov (PTT) Regularization

[11] The linear system of equation (6) is usually ill-posed. The total number of unknown parameters could be larger than the total number of measurements. The number of “independent” measurements will (usually) be even smaller. This ill-posedness can be exactly diagnosed using the singular value decomposition (SVD) of the matrix \mathbf{A} , i.e., $\mathbf{A} = \mathbf{U}\mathbf{D}\mathbf{V}^T$, where $\mathbf{U} \in R^{M \times M}$ and $\mathbf{V} \in R^{N \times N}$ are real and orthogonal matrices and \mathbf{D} is a diagonal matrix whose diagonal elements are the singular values. The exact solution of equation (6) (if it exists) can then be expressed as [*Hansen*, 1992a]

$$\Delta\boldsymbol{\eta} = \sum_{j=1}^N \frac{\mathbf{u}_j^T \Delta\mathbf{I}}{\sigma_j} \mathbf{v}_j, \quad (7)$$

in which \mathbf{u}_j and \mathbf{v}_j are the j th column vector of \mathbf{U} and \mathbf{V} , respectively, and σ_j is the j th singular value. If $\Delta\mathbf{I}$ contains errors and very small or zero (when $M < N$) singular values occur, equation (7) shows that the solution may become unstable or may not exist at all.

[12] To overcome such problem, a number of regularization procedures have been introduced in the literature, such as the Philips–Twomey–Tikhonov (PTT) regularization. A review of these procedures was given by *Hansen* [1992a]. This regularization, sometimes also known as constrained linear inversion [*Twomey*, 1977, section 6.3], has been widely used in many areas. In this paper, we will also develop our inversion algorithm based on this regularization.

[13] The recent development by *Dubovik et al.* [2000] and *Dubovik and King* [2000] should be mentioned here, especially in relation to the handling of measurements with different levels of precision. In that case, they have taken a statistic approach so that measurements with different errors are fitted to different accuracy. In our development, weighted smoothness is also applied, however that is not linked directly with measurement error. It may be advanta-

geous to explore the possibility of linking the two approaches so that our inversion could also take advantage of the merit of the approach by *Dubovik et al.* However, that will require a separate paper. We have also not tried the use of the statistical approach of *Rodgers* [1976], which also might be worth investigating in the future.

[14] Because the radiances are not known exactly, a family of feasible solutions, bounded by the error level, may exist for the original problem. The task of regularization is to pick out the most reasonable one from the feasible solution set. This is achieved by bringing in a priori knowledge about the solution. For example, in the PTT regularization, it is assumed that the solution is smooth in some sense. This assumption is reasonable for a wide range of physical problems, and is true for the problem of our inversion. With this assumption, the original problem could be stated as a constrained extremum problem, which in turn is stated as an equivalent linear system problem [*Twomey*, 1963, 1977, section 6.3]. In general form, this linear system is expressed as

$$(\mathbf{A}^T \mathbf{A} + \gamma \mathbf{H}^T \mathbf{H}) \Delta\boldsymbol{\eta}_{reg} = \mathbf{A}^T \Delta\mathbf{I} + \gamma \mathbf{H}^T \mathbf{H} \Delta\boldsymbol{\eta}_p. \quad (8)$$

In equation (8), $\Delta\boldsymbol{\eta}_{reg}$ is a regularized solution which should ideally be a close approximation to the exact solution, $\Delta\boldsymbol{\eta}$, of equation (6). $\Delta\boldsymbol{\eta}_p$ is called the trial solution; γ is a positive number originating from the Lagrange multiplier of the constrained extremum problem, and is also-called the regularization parameter. The matrix \mathbf{H} , called the smoothing matrix, is used to measure the “smoothness” of the solution. The smoothness can be defined in diverse ways. Among them the norm of the solution vector, the first or second difference [*Twomey*, 1963, 1977, section 6.3] are most frequently used.

[15] As a general form of regularization, equation (8) actually combines the effects of two classes of constraints. Setting $\Delta\boldsymbol{\eta}_p = \mathbf{0}$ leads to a smoothness constraint measured by the solution itself. This type of constraint has found a wide range of applications. Here we are also particularly interested in the second constraint in the equation: the solution is constrained to an independent trial solution. For example, when \mathbf{H} is set to be the identity matrix (\mathbf{I}), equation (8) then has the effect of minimizing

$$\| \Delta\boldsymbol{\eta}_{reg} - \Delta\boldsymbol{\eta}_p \|^2$$

The primary reason that we are particularly interested in the trial solution is due to the fact that the radiance in the whole range of scattering angles usually cannot be obtained from a single instrument. For example, the backscattering part cannot be obtained at the ground. It is found that the trial solution is a good mechanism to provide a reasonable default value for the phase function in the range of scattering angles that are not measured. Also, the trial solution has the effect of maintaining a proper shape of the regularized solution [*Twomey*, 1963]. We will discuss in more detail later the role of the trial solution.

3.2. Characteristics of Aerosol Phase Function Expansion Coefficients

[16] We now present some study results regarding the characteristics of aerosol phase functions. This will be

helpful in the next section when we discuss the selection of the smoothing matrix, \mathbf{H} , the trial model, $\boldsymbol{\eta}_p$, and the determination of the regularization parameter, γ .

[17] It is of great importance for us to study the characteristics of one of the targets of our inversion, the phase function coefficients as a whole. Figure 1 shows two typical curves of aerosol phase function coefficients calculated using Mie theory. Some characteristics of the curves can be identified.

1. All coefficients are positive.
2. If we treat the two-point fluctuations in the lower curve of Figure 1 as “extended smooth,” then the curves have a smooth monodecreasing tail.

[18] A large number of Mie calculations for different aerosol models, refractive indices and wavelengths have shown that these two characteristics always hold. However, it is hard to derive them theoretically. Because of this, a less strict demonstration is provided here. First, the phase function coefficients of a polydispersion system, χ_l , can be expressed as a weighted average of those of a monodispersion system, $\chi_l^{(\text{mono})}$, as

$$\chi_l = \frac{\int_{x_1}^{x_2} \sigma_s^{(\text{mono})}(m, x) \chi_l^{(\text{mono})}(m, x) n(x) dx}{\int_{x_1}^{x_2} \sigma_s^{(\text{mono})}(m, x) n(x) dx}, \quad (9)$$

where $n(x)$ is the size distribution as a function of the size parameter, x , and σ_s is the scattering cross section. The coefficients, $\chi_l^{(\text{mono})}$, can be obtained by expanding the phase function calculated by Mie theory. However, care must be taken to avoid numerical errors. Another more direct and probably more efficient way to calculate $\chi_l^{(\text{mono})}$ was described by *Chu and Churchill* [1955] and *Clark et al.* [1957].

[19] In the case of strong absorption as shown in Figure 2a, all the monodispersion phase function coefficient curves are smooth with a single peak. The magnitude, the order of the maximum term and the total number of effective terms (say, terms larger than 0.1) are approximately linearly related to size parameter. In this case, the averaged phase function from equation (9) will strictly have the characteristics listed above.

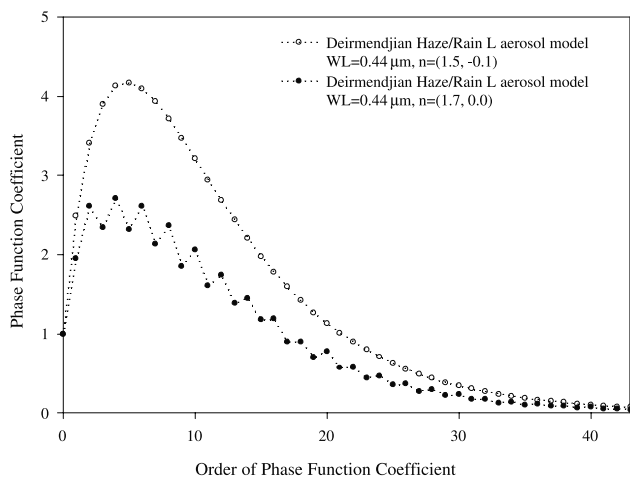


Figure 1. Examples of aerosol phase function Legendre polynomial coefficients showing the typical characteristics of these curves.

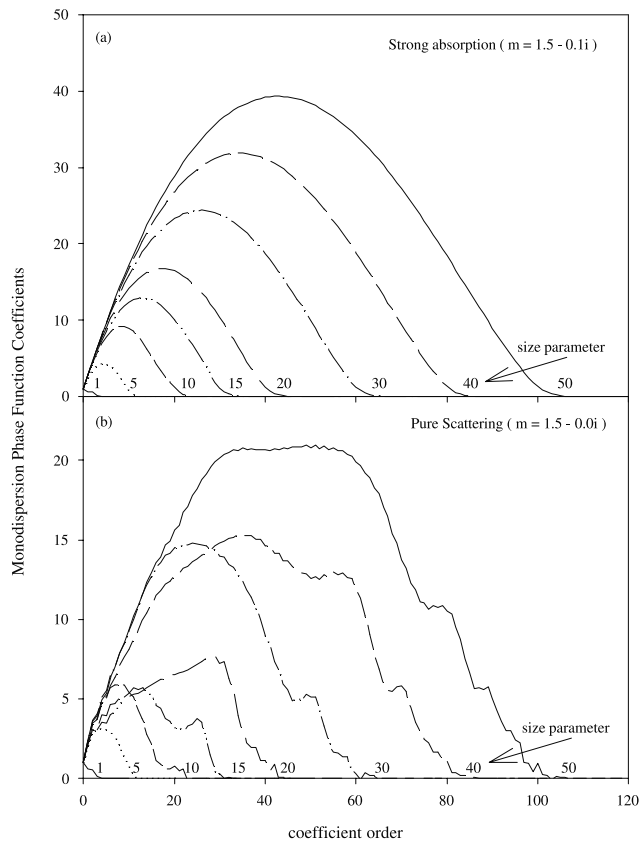


Figure 2. Phase function Legendre polynomial coefficients for monodispersion systems.

[20] However, the situation becomes very complicated in the case of pure scattering or weak absorption as shown in Figure 2b. In such cases the monodispersion coefficient curves have many small spurs. The order and magnitude of the maximum term are no longer strictly related to size parameter. In this case we cannot directly derive the characteristics of the polydispersion phase function coefficient curve. However, it has been found that the monodispersion coefficients are highly variable with size parameter in the case of pure scattering and weak absorption. Because of this, the average taken in equation (9) will almost always smooth out the spurs in the monodispersion curves. A large number of Mie calculations, as mentioned before, have demonstrated this indirectly.

[21] Although what is shown above is for aerosol phase function, the conclusion is applicable to the phase function of the whole atmosphere. The molecular phase function is completely described by three coefficients, i.e., 1.0, 0.0, and 0.5. When it is combined linearly with the aerosol phase function to form the phase function of the whole atmosphere, all but the zeroth- and second-order coefficients will be multiplied by a constant. This does not affect the conclusions already reached. The characteristics of the phase function coefficient curve will be an important guide later in developing our inversion algorithms.

4. Inversion Algorithm

[22] In this section we will discuss all the elements of the regularized problem, equation (8), including the smoothing

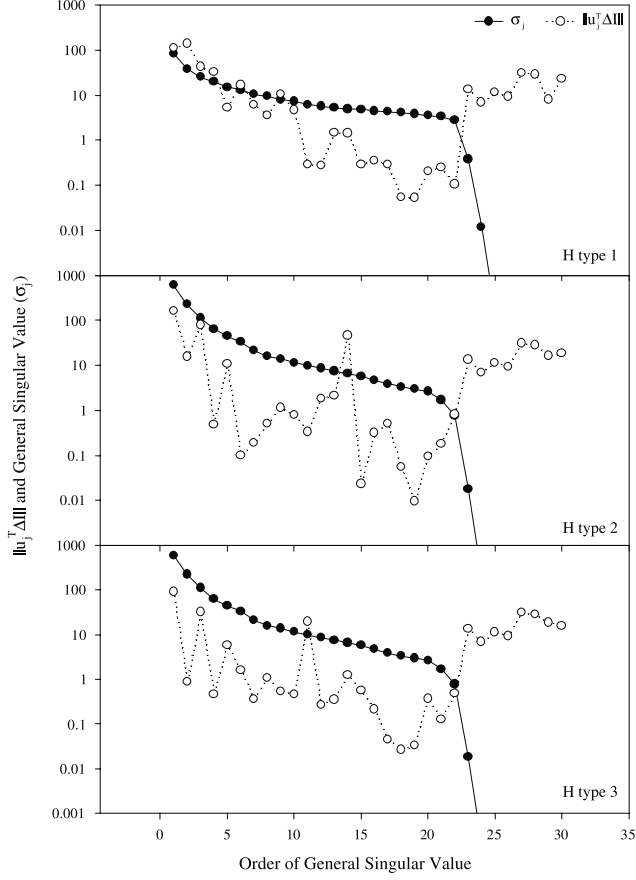


Figure 3. Discrete Picard condition $\|\mathbf{u}_j^T \Delta \mathbf{I}\|$ and general singular values associated with three commonly used smoothing matrices.

matrix, \mathbf{H} , the trial solution, $\Delta \eta_p$, and the regularization parameter, γ .

4.1. Discrete Picard Condition and Smoothing Matrix, \mathbf{H}

[23] In Appendix A, we describe the general singular value decomposition (GSVD). We now briefly introduce the discrete Picard condition that is described in terms of GSVD. If we denote the j th column vector of \mathbf{U} (in equation (A1)) as \mathbf{u}_j , then to ensure that a “smooth” regularized solution exists and that it is a reasonable approximation to the exact solution, the values of $\|\mathbf{u}_j^T \Delta \mathbf{I}\|$ must decay faster, on average, than the general singular values, σ_j . This is the so-called discrete Picard condition [Varah, 1979; Hansen, 1990].

[24] To check this condition, Figure 3 shows the value of $\|\mathbf{u}_j^T \Delta \mathbf{I}\|$ and the general singular values, σ_j , associated with three commonly used smoothing matrices, \mathbf{H} , defined in order that (1) the norm of the regularized solution, $\Delta \eta_{reg}$, is minimized (in this case $\mathbf{H} = \mathbf{I}$); (2) the first-order difference of $\Delta \eta_{reg}$ is minimized; and (3) the second-order difference of $\Delta \eta_{reg}$ is minimized.

[25] The definition of these matrices is given by Twomey [1977, section 6.3]. By comparing the curves in Figure 3 it can be seen that before the measurement error starts to dominate as indicated by the turn-up of $\|\mathbf{u}_j^T \Delta \mathbf{I}\|$, for all three cases, $\|\mathbf{u}_j^T \Delta \mathbf{I}\|$ on average decays faster than σ_j . According to the Picard condition, this indicates the success

of the inversion. By comparing the three cases, we see that $\|\mathbf{u}_j^T \Delta \mathbf{I}\|$ of the first case has the fastest relative decay speed because σ_j in this case decays more slowly than in the other two cases. To obtain a more stable solution, the first type of \mathbf{H} , i.e., the identity matrix, should be used in the inversion. This selection has been justified by numerical experiments. Although it is not directly comparable for results of second and later iterations, it is found that in the case of the first type \mathbf{H} the Picard condition generally improves in successive iterations but this is not the case for the other two choices. Finally we would like to point out that, in the above discussion, the trial solution is not involved. The Picard condition checks only the suitability of the type of smoothness expressed in \mathbf{H} for the particular problem.

[26] Because $\mathbf{H} = \mathbf{I}$ in the first case, the general singular values of the pair (\mathbf{A}, \mathbf{H}) actually equate to the singular values of \mathbf{A} . We see in Figure 3 (\mathbf{H} Type 1) that a distinct gap (sudden drop) exists in the singular value curve. Because such a characteristic is so obvious, we feel it is necessary to check it further since such a characteristic may indicate the success of another regularization method: the truncated singular value decomposition, or TSVD algorithm [Varah, 1979]. The basic idea behind the TSVD is to truncate the summation of equation (7) before the singular values become too small, so as to avoid the dominance of measurement error, i.e.,

$$\Delta \eta_{reg} = \sum_{j=1}^k \frac{\mathbf{u}_j^T \Delta \mathbf{I}}{\sigma_j} \mathbf{v}_j, \quad (10)$$

where $k < N$. This truncated summation is actually a regularized solution. However, the behavior of this method strongly depends on the selection of k , which plays a role similar to γ in the PTT regularization. Intuitively, we would choose k right before the gap of the singular values: for example, $k = 22$ in the case of Figure 3. Unfortunately, numerical testing has found that k chosen in this way is still too large to effectively suppress the influence of measurement error. Because of this, we did not take this approach in our inversion but we give this brief discussion in order to avoid possible concerns.

4.2. Determination of the Regularization Parameter

[27] Having selected the smoothing matrix, \mathbf{H} , we now turn to the determination of the regularization parameter, γ . Because iteration is used, it is critically important to derive the proper value of γ so that stability can be maintained in successive iterations. In sections 4.2.1 and 4.2.2, we will present two attempts regarding the determination of this parameter.

[28] In the literature, a number of methods have been proposed to determine the regularization parameter. Among them are general cross-validation (GCV) [Golub et al., 1979], the discrepancy principle [Morozov, 1974, section 10; Groetsch, 1984], quasi-optimality criterion [Morozov, 1974, section 27], and the method suggested by Strand and Westwater [1968]. Another method we would particularly like to mention is the so-called L curve method [Hansen, 1992a, 1992b], which has succeeded in a number of applications [Schimpf and Schreier, 1997; Liu et al., 1999] and is becoming quite popular.

[29] Unfortunately, it was found that in our inversion the value of γ determined by the L curve method is consistently too small to effectively suppress the strong oscillations in the solution. Consequently, the reconstructed phase function is also highly oscillatory, or even becomes negative at some angles. The overall iteration could not continue in some cases due to numerical problems. Numerical examples will be given in paper 2 to illustrate this. We have also checked the general cross-validation method and it is found that it produces a γ value close to that of the L curve method. As for the discrepancy principle and quasi-optimality criterion, *Hansen* [1992b] has discussed how these methods should also give similar values to the L curve method, and thus we will not check them again here.

[30] The reason that these methods do not work well in our inversion probably is that these methods have put more emphasis on maximizing information utilization rather than sufficiently suppressing the influence of measurement error. This might have resulted in a biased regularization parameter. In a case where the problem is solved once off, this may be a very desirable property. However, the exact reason is still not clear and must be investigated later. The assumptions made by these methods must also be carefully checked. For example, these methods assume the left-hand side, i.e., \mathbf{A} , does not have any error. Obviously, because of kernel approximation in our inversion, the matrix \mathbf{A} definitely does not satisfy this assumption.

[31] Because these methods could not provide the proper regularization parameter, we have to explore other possibilities. Before doing so, we firstly apply the general singular value decomposition (GSVD, see Appendix A) to the regularized problem (equation (8)). The regularized solution is then expressed in terms of the regularization parameter, γ , and the components of the GSVD:

$$\Delta\eta_{reg} = \mathbf{XWU}^T\Delta\mathbf{I} + \mathbf{XW}_p\mathbf{X}^{-1}\Delta\eta_p, \quad (11)$$

in which

$$\mathbf{W} = \begin{bmatrix} \mathbf{I}_K & \\ & \text{diag}(f_j/\alpha_j, j = K+1 \dots \min(K+L, M)) \\ & & \mathbf{\Omega} \end{bmatrix}, \quad (12)$$

$$\mathbf{W}_p = \begin{bmatrix} \mathbf{0}_K & \\ & \text{diag}(1 - f_j, j = K+1 \dots \min(K+L, M)) \\ & & \mathbf{\Xi} \end{bmatrix}, \quad (13)$$

$$f_j = \frac{\sigma_j^2}{\sigma_j^2 + \gamma}, \quad (14)$$

$$\mathbf{\Omega} = \begin{cases} \mathbf{0}_{M-(K+L)} & (M > K+L) \\ \text{null} & (M \leq K+L) \end{cases} \quad \mathbf{\Xi} = \begin{cases} \text{null} & (M > K+L) \\ \mathbf{I}_{K+L-M} & (M \leq K+L) \end{cases} \quad (15)$$

where \mathbf{I}_x is an x by x identity matrix, $\mathbf{0}_x$ is an x by x zero matrix, and null means that part does not exist. *Hansen* [1992b] has derived similar expressions with the assumption that the number of measurements is more than the number of unknowns. We have to remove this restriction because the assumption is not always true in our case.

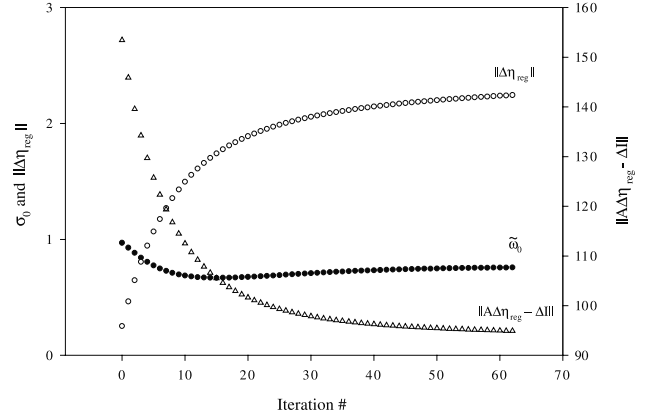


Figure 4. Stabilizing of $\tilde{\omega}_0$, $\|\Delta\eta_{reg}\|$, and $\|\mathbf{A}\Delta\eta_{reg} - \Delta\mathbf{I}\|$ when approaching the optimum solution in the preset gamma algorithm.

4.2.1. Preset Gamma Algorithm

[32] Equation (14) shows that on the one hand, the regularization parameter, γ , suppresses the influence of measurement error in the case of small general singular values, σ_j . On the other hand, it balances the contributions made by the measurement and the trial solution. Accordingly, the value of γ should be decided by the measurement error and the similarity of the trial solution to the true solution: (1) larger measurement error requires larger γ ; and (2) the farther away the trial solution is from the true solution, the less weight should be given to the trial solution, or a smaller γ should be used.

[33] Thinking in reverse, it can also be stated that the larger γ is, the closer the trial solution must be to the true solution so that it really “deserves” the large γ . In the extreme case, if γ is set to a very large value, then the trial solution must be sufficiently close to the true value, that is,

$$\Delta\eta_{reg} \approx \mathbf{XWU}^T\Delta\mathbf{I} + \mathbf{XW}_p\mathbf{X}^{-1}\Delta\eta_{reg}. \quad (16)$$

So rather than trying to find a proper γ for a given trial solution, we preset γ to a sufficiently large value and then try to find the proper trial solution; such a trial solution must satisfy equation (16). We refer to this method as the “preset gamma algorithm” due to the use of the large preset γ .

[34] Because equation (16) itself is ill-posed, instead of solving it directly, it can be solved iteratively as

$$\Delta\eta_{reg}^{(n+1)} = \mathbf{XWU}^T\Delta\mathbf{I} + \mathbf{XW}_p\mathbf{X}^{-1}\Delta\eta_{reg}^{(n)} \quad (17)$$

$$\Delta\eta_{reg}^{(1)} = \Delta\eta_p,$$

where $\Delta\eta_p$ is the initial trial solution. This trial solution is improved in successive iterations by adding more contribution from the measurement.

[35] The problem now is to find the criteria to terminate this iteration. Figure 4 shows the single scattering albedo, $\tilde{\omega}_0$, the norm of the solution, $\|\Delta\eta_{reg}\|$, and the norm of the residual, $\|\mathbf{A}\Delta\eta_{reg} - \Delta\mathbf{I}\|$. All are plotted against the iteration index. All these curves show a stable state of flat level, which may indicate the time of terminating the iteration. By studying numerical experiment results, the

following criteria have been selected: (1) the change of single scattering albedo in two successive iterations is sufficiently small and (2) the number of simple smooth sections (see below) in the phase function coefficient curve starts to increase.

[36] For the moment, only the single scattering albedo is used as a criterion. We feel more study is necessary to make use of the state of these values. In the second criterion, by “simple smooth section” we mean an ascending or descending section of the coefficient curve that is longer than, say 5 points. Before starting the iteration, the preset gamma (e.g., $\gamma = 10^4$) is so large that the solution is totally dominated by the trial solution, the number of simple smooth sections should be (usually) 2 (recall Figure 1). As the iteration progresses, malformations start to appear in the solution curve because more and more contribution from the (error-contaminated) measurements is added to the intermediate solution. The solution at the n th iteration is shown in the following equation, derived by applying the iteration of equation (17) analytically:

$$\Delta\eta_{\text{reg}}^{(n)} = (\mathbf{I} - \mathbf{P})^{-1}(\mathbf{I} - \mathbf{P}^n)\mathbf{X}\mathbf{W}\mathbf{U}^T\Delta\mathbf{I} + \mathbf{P}^n\Delta\eta_p \quad (18)$$

$$\mathbf{P}^n = \mathbf{X}\mathbf{W}^n\mathbf{X}^{-1}.$$

The second criterion actually serves as a safeguard to avoid unstable iteration. Numerical examples will be given by Qin *et al.* [2002b] to illustrate the behavior of this method.

4.2.2. Variable Gamma Algorithm

[37] While conducting numerical experiments, it has been observed that the higher-order terms of the regularized solution, η_{reg} from equation (11), tend to suffer more from measurement error than the lower-order terms. To illustrate this, η_{reg} was first calculated using equation (11) for a range of γ from 0.1 to 1000. The results were then divided into two parts, from where the corresponding general singular values start to drop down rapidly (see Figure 3). Finally the norm of the difference between η_{reg} and the true value η , $\|\eta_{\text{reg}}(\text{first part}) - \eta(\text{first part})\|$ and $\|\eta_{\text{reg}}(\text{second part}) - \eta(\text{second part})\|$ for the two parts, are plotted in Figure 5b and are labeled “first part fixed γ ” and “second part fixed γ ”, respectively. It can be seen that the optimum γ for the first part, or the γ value which minimizes $\|\eta_{\text{reg}}(\text{first part}) - \eta(\text{first part})\|$, is about 50 in this case, while the optimum γ for the second part is about 250.

[38] The difference between the two γ indicates that a single fixed γ might not be able to optimize the solution for all orders and thus some sort of variable γ becomes necessary. After extensive numerical experiment, the following expression is defined to substitute γ in equation (14) by $\tilde{\gamma}$:

$$\tilde{\gamma}_i = \frac{\|\mathbf{x}_i\|}{\|\mathbf{x}_1\|}\gamma, i = 1, 2, \dots, N, \quad (19)$$

where \mathbf{x}_i is the i th column vector of \mathbf{X} . The solution after this substitution is denoted as $\tilde{\eta}_{\text{reg}}$. Figure 5a shows an example of the factor $\|\mathbf{x}_j\|/\|\mathbf{x}_1\|$. Note that $\tilde{\eta}_{\text{reg}}$ is still a function of γ but the meaning of this γ is now different. As in the case of fixed γ , $\|\eta_{\text{reg}}(\text{first part}) - \eta(\text{first part})\|$ and $\|\eta_{\text{reg}}(\text{second part}) - \eta(\text{second part})\|$ are also plotted in Figure 5b and are labeled as “first part variable γ ” and “second part variable γ ”, respectively.

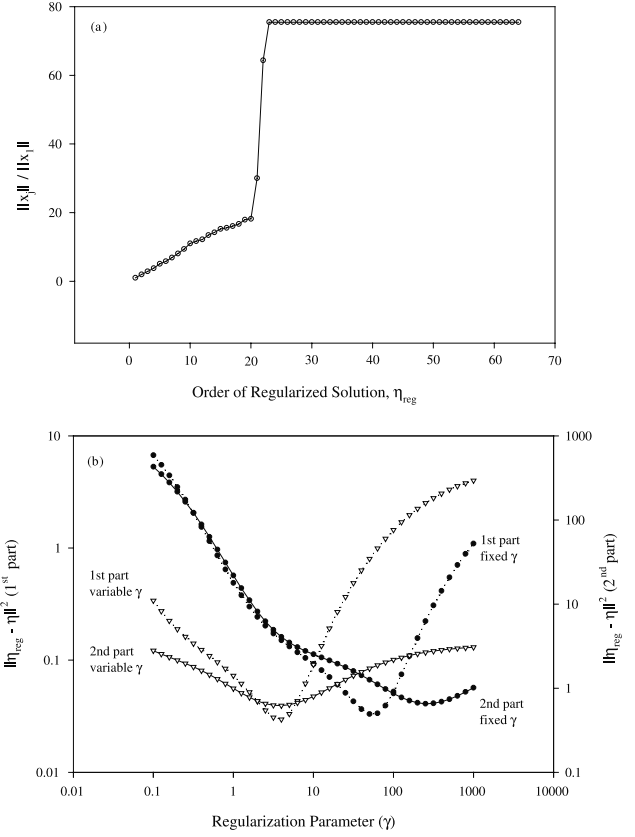


Figure 5. (a) Example of γ adjustment factor $\|\mathbf{x}_j\|/\|\mathbf{x}_1\|$. See text for detailed explanation. (b) The different effects of regularization parameter on the regularized solution’s lower-order and higher-order terms and the necessity to adjust the regularization parameter.

“second part variable γ .” Indeed it can be seen that after the substitution of γ in equation (14), the optimum γ for the two parts are now almost the same, and the impact of measurement error is now well balanced for all the phase function coefficients.

[39] However, the γ in equation (19) is yet to be decided. When we gradually increase γ from a very small value, it can be observed that the fluctuation in the solution, $\tilde{\eta}_{\text{reg}}$, is reduced gradually – the movement of different parts of the curve is in opposite directions toward an “average” state: the optimum solution. During this process, the number of simple sections is also reduced gradually. However, increasing γ excessively will only move the whole curve in one direction, the direction toward the trial solution. In the mean time, the number of simple sections no longer decreases. On the basis of this observation, a number of values have been defined and tested to measure the smoothness of the solution, so that a criterion can be defined to determine the γ of equation (19). It is found that the “number of simple sections” is a really simple but most reliable indication of “optimum” damping. Specifically, we choose the minimum γ which generates the minimum number of simple smooth sections in the reasonable range of γ . Because of the use of the variable gamma, we refer this method as the variable gamma algorithm.

[40] Finally, we would like to point out that γ is a relative value. From equation (8) it is seen that gamma is propor-

tional to the absolute magnitude of the radiance. Also, different problems may have different γ . Because of this, care must be taken when comparing values from different sources.

4.3. Trial Solution

[41] In this section, we will check the trial solution. When starting the overall iteration, a reasonable choice of the trial model is the base model, which usually is the best guess we have. In successive iterations, we have two options: (1) updating the trial model together with the base model and (2) retaining the initial trial model.

[42] If the trial model is updated with the new base model, it will get closer to the true value, and thus the regularization parameter γ is “encouraged” to become larger. Intuitively we have taken the first option in our early attempts, hoping that the larger γ suppresses measurement error more effectively. However, in this case, errors in the new base model, due to errors in the measurement, will be passed on to the trial model. The error is thus accumulated in successive iterations.

[43] Instead of updating the trial model in successive iterations, our numerical experiments have shown that sticking to a fixed trial solution is more reliable, especially when strong noise is present. In this case, γ will roughly stay at a steady level in successive iterations. In our inversion, we have updated the single scattering albedo of the trial model in successive iterations, but the phase function is kept unchanged. It is possible to construct a more sophisticated algorithm; for example, we may fit the new base model to an analytical model and use the fitted model as the new trial model. In this way, the trial model is, to some extent, brought closer to the true solution. In the mean time, the trial model is also free of undesirable malformation due to error accumulation. We leave this refinement for future work.

[44] As already mentioned, the trial model provides us the mechanism to supplement a more reasonable default value for the range of scattering angles not covered by the measurements. This is the problem we always have to face since it is unlikely that we can measure the whole range of scattering angles simultaneously on ground alone. From equation (11) it is straightforward to show that

$$\Delta \mathbf{S} = \mathbf{P}\mathbf{X} \left(\mathbf{W}\mathbf{U}^T \Delta \mathbf{I} + \mathbf{W}_p (\mathbf{P}\mathbf{X})^{-1} \Delta \mathbf{S}_p \right), \quad (20)$$

where \mathbf{S} denotes the scattering function, the multiplication of phase function by the single scattering albedo. \mathbf{P} is a matrix with row vectors being the Legendre polynomial of given scattering angles such that $\mathbf{S} = \mathbf{P}\boldsymbol{\eta}$.

[45] This expression shows that the regularized solution is a linear combination of the exact solution and the trial solution. The contributions from the two components are adjusted by the regularization parameter, γ , contained in \mathbf{W} and \mathbf{W}_p (equations (12)–(14)). Generally speaking, γ should fall into the range that, on the upper end, it is smaller than the value that causes the solution to bias to the trial solution (in the range of scattering angles where measurements are available) and on the lower end, it is big enough to suppress the influence of measurement error. The extreme situation is that the measurement is totally domi-

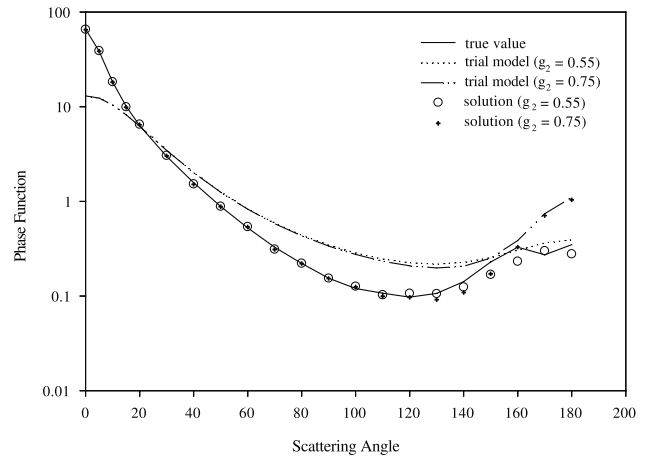


Figure 6. Role of the trial model in providing default values for the part of phase function that is not covered by measurement.

nated by error. In that case, γ becomes so large that the solution finally slides back to the trial solution. When the measurement is not available, which means no contribution comes from the measurement, the solution will be dominated by the trial solution.

[46] To illustrate the effect of trial solution in supplying a default value for the range of unmeasured scattering angles, Figure 6 shows two retrieved phase functions from the same set of simulated sky radiances, but using two different trial phase functions. The two trial phase functions used are in the form of two-term Henyey-Greenstein (TTHG) functions defined as [Kattawar, 1975]

$$P(\alpha, g_1, g_2, \Theta) = \alpha \frac{1 - g_1^2}{1 + g_1^2 - 2g_1 \cos(\Theta)} + (1 - \alpha) \frac{1 - g_2^2}{1 + g_2^2 + 2g_2 \cos(\Theta)}, \quad (21)$$

where Θ is the scattering angle. The parameters of the two trial phase functions are $\alpha = 0.965$, $g_1 = 0.65$, $g_2 = 0.55$ and $\alpha = 0.965$, $g_1 = 0.65$, $g_2 = 0.75$, respectively. The true phase function, calculated for the Deirmendjian Haze M aerosol model [McCartney, 1976] at wavelength $\lambda = 0.67 \mu\text{m}$ and assumed refractive index $n = (1.41, -0.002)$, is also plotted in Figure 6. In this case, the measurement is an almucantar circle with the Sun at zenith angle 55° . The largest measurable scattering angle is thus 110° . We can see that in the range of $0^\circ \sim 110^\circ$, the retrieved phase functions follow the true phase function very well, because in this part they are controlled by the measurements. However, from 110° the retrieved phase functions start to move away from the true phase function and toward the trial models. By 180° , the retrieved phase functions are dominated by the trial phase functions. Example results retrieved from real CIMEL data in the second paper also show such features.

5. Summary

[47] A linear relation has been introduced which approximately links the perturbation of the scattering function (the

multiplication of single scattering albedo and phase function), in the form of a Legendre polynomial expansion, to the difference between sky radiances measured at multiple angles and the base model radiances at corresponding angles.

[48] Because the established linear system is usually ill-posed, regularization is required to obtain a stable solution which approximates the true solution. In this paper, the Philips–Twomey–Tikhonov regularization has been adopted to develop our inversion procedure. All the components of the regularization have been discussed in this paper.

[49] A key and difficult step in applying the above regularization is the determination of the regularization parameter, especially when an iterative procedure has been used in the inversion. In this paper, efforts have been made to obtain this value. In the first method, referred to as the preset gamma algorithm, the single scattering albedo, the solution norm and the residual norm all reach a stable flat level, which indicate the potential for success. The other method that is developed, referred to as the variable gamma algorithm, introduces an adjustment to the regularization parameter, which balances the influence of measurement error on different orders of the phase function coefficients. *Qin et al.* [2002b] will apply both methods to synthetic data to check their applicability.

[50] *Qin et al.* [2002b] apply the developed algorithm to CIMEL measurements as well as simulated sky radiances. Assumptions made in this algorithm, such as assumptions about the surface albedo and the optical thickness, are also checked.

Appendix A. General Singular Value Decomposition (GSVD)

[51] The singular value decomposition (SVD) has been used to diagnose linear system problems. The GSVD is another mathematical tool that allows us to look into the regularized problem of equation (8) [*Hansen*, 1992a, 1992b]. Briefly, for a pair of real matrices (\mathbf{A} , \mathbf{H}), $\mathbf{A} \in R^{M \times N}$, $\mathbf{H} \in R^{N \times N}$, a decomposition exists such that [*Bai and Demmel*, 1993]

$$\begin{aligned} \mathbf{A} &= \mathbf{U}\mathbf{D}_1\mathbf{X}^{-1} \\ \mathbf{H} &= \mathbf{V}\mathbf{D}_2\mathbf{X}^{-1}, \end{aligned} \quad (\text{A1})$$

in which $\mathbf{U} \in R^{M \times M}$, $\mathbf{V} \in R^{N \times N}$ are orthonormal, i.e., $\mathbf{U}^T\mathbf{U} = \mathbf{I}$ and $\mathbf{V}^T\mathbf{V} = \mathbf{I}$, and $\mathbf{X} \in R^{N \times N}$ is a full rank matrix. Let $K + L$ equal the effective numerical rank of $(\mathbf{A}^T, \mathbf{H}^T)^T$. In our work, the matrix \mathbf{H} will be selected so that $K + L$ will always equal N , the number of unknowns. In equation (A1), $\mathbf{D}_1 \in R^{M \times N}$, $\mathbf{D}_2 \in R^{N \times N}$. When $M \geq N$,

$$\mathbf{D}_1 = \begin{bmatrix} \mathbf{I}_K & 0 \\ 0 & \mathbf{C} \\ 0 & 0 \end{bmatrix}, \quad \mathbf{D}_2 = \begin{bmatrix} 0 & \mathbf{S} \\ 0 & 0 \end{bmatrix}, \quad (\text{A2})$$

or when $M < N$,

$$\mathbf{D}_1 = \begin{bmatrix} \mathbf{I}_K & 0 & 0 \\ 0 & \mathbf{C} & 0 \end{bmatrix}, \quad \mathbf{D}_2 = \begin{bmatrix} 0 & \mathbf{S} & 0 \\ 0 & 0 & \mathbf{I}_{K+L-M} \\ 0 & 0 & 0 \end{bmatrix}, \quad (\text{A3})$$

where

$$\begin{aligned} \mathbf{C} &= \text{diag}(\alpha_{K+1}, \alpha_{K+2}, \dots, \alpha_{\min(M,N)}), \\ \mathbf{S} &= \text{diag}(\beta_{K+1}, \beta_{K+2}, \dots, \beta_{\min(M,N)}), \\ \alpha_j^2 + \beta_j^2 &= 1, j = K + 1, K + 2, \dots, \min(M, N). \end{aligned} \quad (\text{A4})$$

The general singular values are then defined as

$$\sigma_j = \alpha_j / \beta_j, j = K + 1, K + 2, \dots, \min(M, N), \quad (\text{A5})$$

which are equal to the singular values of \mathbf{A} in case $\mathbf{H} = \mathbf{I}$. Fortran source code for GSVD is available in LAPACK. (This library and documentation are available at <http://www.netlib.org/>.)

[52] The solution of equation (8) can be obtained using the GSVD. Note that

$$\begin{aligned} \mathbf{A}^T &= (\mathbf{X}^{-1})^T \mathbf{D}_1^T \mathbf{U}^T \\ \mathbf{H}^T &= (\mathbf{X}^{-1})^T \mathbf{D}_2^T \mathbf{V}^T \end{aligned} \quad (\text{A6})$$

and also that \mathbf{U} and \mathbf{V} are orthonormal. We can then express equation (8) as

$$\begin{aligned} &(\mathbf{X}^{-1})^T (\mathbf{D}_1^T \mathbf{D}_1 + \gamma \mathbf{D}_2^T \mathbf{D}_2) \mathbf{X}^{-1} \Delta \eta_{\text{reg}} \\ &= (\mathbf{X}^{-1})^T \mathbf{D}_1^T \mathbf{U}^T \Delta \mathbf{I} + \gamma (\mathbf{X}^{-1})^T \mathbf{D}_2^T \mathbf{D}_2 \mathbf{X}^{-1} \Delta \eta_p. \end{aligned} \quad (\text{A7})$$

If we left multiply both sides by $\mathbf{X}(\mathbf{D}_1^T \mathbf{D}_1 + \gamma \mathbf{D}_2^T \mathbf{D}_2)^{-1} \mathbf{X}^T$ and note that $\mathbf{X}^T(\mathbf{X}^{-1})^T = (\mathbf{X}^{-1}\mathbf{X})^T = \mathbf{I}$, we have

$$\Delta \eta_{\text{reg}} = \mathbf{X}\mathbf{W}\mathbf{U}^T \Delta \mathbf{I} + \mathbf{X}\mathbf{W}_p \mathbf{X}^{-1} \Delta \eta_p, \quad (\text{A7}')$$

where

$$\begin{aligned} \mathbf{W} &= (\mathbf{D}_1^T \mathbf{D}_1 + \gamma \mathbf{D}_2^T \mathbf{D}_2)^{-1} \mathbf{D}_1^T \\ \mathbf{W}_p &= (\mathbf{D}_1^T \mathbf{D}_1 + \gamma \mathbf{D}_2^T \mathbf{D}_2)^{-1} (\gamma \mathbf{D}_2^T \mathbf{D}_2). \end{aligned} \quad (\text{A8})$$

We now expand equation (A9) for the case $M < N$ to obtain the expressions for \mathbf{W} and \mathbf{W}_p (The other case can be done similarly). We note that

$$\mathbf{D}_1^T \mathbf{D}_1 = \begin{bmatrix} \mathbf{I}_K & 0 & 0 \\ 0 & \mathbf{C}^2 & 0 \\ 0 & 0 & 0 \end{bmatrix}, \quad \mathbf{D}_2^T \mathbf{D}_2 = \begin{bmatrix} 0 & 0 & 0 \\ 0 & \mathbf{S}^2 & 0 \\ 0 & 0 & \mathbf{I}_{K+L-M} \end{bmatrix}, \quad (\text{A9})$$

and that both $\mathbf{D}_1^T \mathbf{D}_1$ and $\mathbf{D}_2^T \mathbf{D}_2$, and thus $\mathbf{D}_1^T \mathbf{D}_1 + \gamma \mathbf{D}_2^T \mathbf{D}_2$ also are diagonal, their inverse is obtained by inverting each of the diagonal elements. We thus have

$$\begin{aligned} \mathbf{W} &= \begin{bmatrix} \mathbf{I}_K & 0 \\ 0 & (\mathbf{C}^2 + \gamma \mathbf{S}^2)^{-1} \mathbf{C} \\ 0 & 0 \end{bmatrix}, \\ \mathbf{W}_p &= \begin{bmatrix} 0 & 0 & 0 \\ 0 & \gamma (\mathbf{C}^2 + \gamma \mathbf{S}^2)^{-1} \mathbf{S}^2 & 0 \\ 0 & 0 & \mathbf{I}_{K+L-M} \end{bmatrix}. \end{aligned} \quad (\text{A10})$$

Using equation (A4), we can then obtain equations (11)–(15).

[53] **Acknowledgments.** This work was supported by the Earth Observation Center, CSIRO, Australia and Australian International Post-graduate Research Scholarship (IPRS) program.

References

- Bai, Z. J., and J. W. Demmel, Computing the generalized singular value decomposition, *SIAM J. Sci. Comput.*, 14, 1464–1486, 1993.
- Box, M. A., Radiative perturbation theory: A review, *Environ. Model. Software*, 17, 95–106, 2002.
- Box, M. A., and C. Sendra, Retrieval of the albedo and phase function from exiting radiances with radiative perturbation theory, *Appl. Opt.*, 38, 1636–1643, 1999.
- Box, M. A., S. A. W. Gerstl, and C. Simmer, Application of the adjoint formulation to the calculation of atmospheric radiative effects, *Beitr. Phys. Atmos.*, 61, 303–311, 1988.
- Box, M. A., S. A. W. Gerstl, and C. Simmer, Computation of atmospheric radiative effects via perturbation theory, *Beitr. Phys. Atmos.*, 62, 193–199, 1989a.
- Box, M. A., B. Croke, S. A. W. Gerstl, and C. Simmer, Application of the perturbation theory for atmospheric radiative effects: Aerosol scattering atmospheres, *Beitr. Phys. Atmos.*, 62, 200–211, 1989b.
- Box, M. A., P. E. Loughlin, M. Samaras, and T. Trautmann, Application of radiative perturbation theory to changes in absorbing gas, *J. Geophys. Res.*, 102, 4333–4342, 1997.
- Charlson, R. J., S. E. Schwartz, J. M. Hales, R. D. Cess, J. A. Coakley, J. E. Hansen, and D. J. Hofman, Climate forcing by anthropogenic aerosols, *Science*, 255, 423–430, 1992.
- Chu, C. M., and S. W. Churchill, Representation of the angular distribution of radiation scattered by a spherical particle, *J. Opt. Soc. Am.*, 45, 958–962, 1955.
- Clark, G. C., C. M. Chu, and S. W. Churchill, Angular distribution coefficients for radiation scattered by a spherical particle, *J. Opt. Soc. Am.*, 47, 81–84, 1957.
- Dubovik, O., and M. D. King, A flexible inversion algorithm for retrieval of aerosol optical properties from Sun and sky radiance measurements, *J. Geophys. Res.*, 105, 20,673–20,696, 2000.
- Dubovik, O., A. Smirnov, B. N. Holben, M. D. King, Y. J. Kaufman, T. F. Eck, and I. Slutsker, Accuracy assessments of aerosol optical properties retrieved from Aerosol Robotic Network (AERONET) Sun and sky radiance measurements, *J. Geophys. Res.*, 105, 9791–9806, 2000.
- Golub, G. H., M. Heath, and G. Wahba, Generalized cross-validation as a method for choosing a good ridge parameter, *Technometrics*, 21, 215–223, 1979.
- Groetsch, C. W., *The Theory of Tikhonov Regularization for Fredholm Equations of the First Kind*, Pitman, London, 1984.
- Hansen, P. C., The discrete Picard condition for discrete ill-posed problems, *BIT*, 30, 658–672, 1990.
- Hansen, P. C., Numerical tools for analysis and solution of Fredholm integral equations of the first kind, *Inverse Problems*, 8, 849–872, 1992a.
- Hansen, P. C., Analysis of discrete ill-posed problems by means of the L curve, *SIAM Rev.*, 34, 561–580, 1992b.
- Holben, B. N., V. Kalb, Y. J. Kaufman, D. Tanre, and E. Vermote, Aerosol retrieval over land from AVHRR data—Application for atmospheric correction, *IEEE Trans. Geosci. Remote Sens.*, 30, 212–222, 1992.
- Holben, B. N., et al., AERONET-A federated instrument network and data archive for aerosol characterization, *Remote Sens. Environ.*, 66, 1–16, 1998.
- Kattawar, G. W., A three-parameter analytic phase function for multiple scattering calculations, *J. Quant. Spectrosc. Radiant. Transfer*, 839–849, 1975.
- Liou, K. N., *An Introduction to Atmosphere Radiation*, Academic, San Diego, Calif., 1980.
- Liu, Y., W. P. Arnott, and J. Hallett, Particle size distribution retrieval from multispectral optical depth: Influence of particle nonsphericity and refractive index, *J. Geophys. Res.*, 104, 31,753–31,762, 1999.
- McCartney, E. J., *Optics of the Atmosphere: Scattering by Molecules and Particles*, John Wiley, New York, 1976.
- Morozov, V. A., *Methods for Solving Incorrectly Posed Problems*, Springer-Verlag, New York, 1974.
- Nakajima, T., G. Tonna, R. Rao, and P. Boi, Use of sky brightness measurements from ground for remote sensing of particulate polydispersions, *Appl. Opt.*, 35, 2672–2686, 1996.
- Qin, Y., D. L. B. Jupp, and M. A. Box, Extension of the discrete-ordinate algorithm and efficient radiative transfer calculation, *J. Quant. Spectrosc. Radiat. Transfer*, 74, 767–781, 2002a.
- Qin, Y., D. L. B. Jupp, and M. A. Box, Inversion of multiangle sky radiance measurement for the retrieval of atmospheric optical properties, 2, Application, *J. Geophys. Res.*, 107, doi:10.1029/2001JD000946, in press, 2002b.
- Rodgers, C. D., Retrieval of atmospheric temperature and composition from remote measurements of thermal radiation, *Rev. Geophys.*, 14, 609–624, 1976.
- Schimpf, B., and F. Schreier, Robust and efficient inversion of vertical sounding atmospheric high-resolution spectra by means of regularization, *J. Geophys. Res.*, 102, 16,037–16,055, 1997.
- Sendra, C., Retrieval of the aerosol scattering parameters using radiative perturbation theory, Ph.D. thesis, Univ. of New South Wales, Kensington, Australia, 1996.
- Sendra, C., and M. A. Box, Retrieval of the phase function and scattering optical thickness of aerosols: A radiative perturbation theory application, *J. Quant. Spectr. Rad. Trans.*, 64, 499–515, 2000.
- Strand, O. N., and E. R. Westwater, Statistical estimation of the numerical solution of a Fredholm integral equation of the first kind, *J. Assoc. Comput. Mach.*, 15, 100–114, 1968.
- Twomey, S., On the numerical solution of Fredholm integral equations of the first kind by the inversion of the linear system produced by quadrature, *J. Assoc. Comput. Mach.*, 10, 97–101, 1963.
- Twomey, S., *Introduction to the Mathematics of Inversion in Remote Sensing and Indirect Measurements*, Dev. Geomath., vol. 3, Elsevier Sci., New York, 1977.
- Varah, J. M., Practical examination of some numerical methods for linear discrete ill-posed problems, *SIAM Rev.*, 21, 100–111, 1979.
- Wang, M. H., and H. R. Gordon, Retrieval columnar aerosol phase function and single-scattering albedo from sky radiance over the ocean: Simulations, *Appl. Opt.*, 32, 4598–4609, 1993.
- Yang, H. Y., and H. R. Gordon, Retrieval of the columnar aerosol phase function and single-scattering albedo from sky radiance over land: Simulations, *Appl. Opt.*, 37, 978–997, 1998.

M. A. Box and Y. Qin, School of Physics, University of New South Wales, Sydney, NSW 2052, Australia. (mab@newt.phys.unsw.edu.au)
D. L. B. Jupp, Earth Observation Center, CSIRO, Canberra, ACT 2601, Australia.